http://ansinet.com/itj

ITJ

ISSN 1812-5638

INFORMATION TECHNOLOGY JOURNAL

ANSInet
Asian Network for Scientific Information
308 Lasani Town, Sargodha Road, Faisalabad - Pakistan

Information Technology Journal 8 (4): 551-557, 2009
ISSN 1812-5638

Analysis of the Constraints and Effects of Frequency Source Noise on High-resolution DBS Imaging

Xie Xianming and Pi Yiming
College of Electronic Engineering, University of Electronic Science and Technology, Chengdu, China

Abstract: Doppler Beam Sharpening (DBS) technique is one of high-resolution radar imaging technique. DBS images are widely used in tactical reconnaissance, terrain matching and navigation, as well as target identification, etc. Range walking correction technique and azimuth dechirping technique can increase the coherent accumulated time of DBS imaging system, which provides greater space for high-resolution DBS Imaging. However, the resolution of DBS images will be limited by frequency source phase noise. This study addresses the effects of frequency source phase noise on the high-resolution DBS imaging. Quantitative estimates are derived analytically based on the second-order statistics characteristic of oscillator phase noise. The research results could further consummate high-resolution DBS imaging theory and provide theory basis for DBS imaging system design.

Key words: High-resolution DBS imaging, frequency source noise, phase errors

INTRODUCTION

Doppler Beam Sharpening (DBS) images can provide reference for the location of the moving target detected by radar to strike more accurately and effectively (Tobin, 1996; Cheng and Sun, 2000; Qi and Zhuizhen, 2004). DBS technique also can be used in trajectory navigation, landform matching, etc. It is widely used in military and economy areas (Zhou, 1988; Zhang, 1991; Mao and Shaohong, 2000). It has been accepted in radar research field because of its less computational load, real-time processing ability and validity (Gerhard and Younis, 2006; Younis *et al*., 2006). The conventional DBS imaging is similar to unfocused SAR (Synthetic Aperture Radar imaging) processing. In these studies, such as study of Wang and Song (2005), Wei and Wen (2005) and Li *et al*. (2006) focused SAR processing methods including range walking correction technique and azimuth dechirping technique were applied to DBS imaging, which could increase coherent accumulated time and improve the resolution of DBS images. However, does it mean that DBS imaging system with a long coherent accumulated time are able to obtain high-resolution DBS images? In fact, due to frequency source phase noise, the longer coherent accumulated time may result in the larger azimuth shift and the bigger broadening of impulse response, as well as stronger spurious sidelobes. But, the effects of frequency source phase noise on high-resolution DBS imaging had been never fully considered in earlier studies. In this study, quantitative estimates are derived analytically and requirement for coherent accumulated time is deduced based on the second-order statistics characteristic of oscillator phase noise.

PHASE NOISE DESCRIPTION AND CHARACTERISTIC

Generally, an oscillator phase noise $\phi(t)$ is regarded as a second-order stationary stochastic process, which is conveniently characterized in the fourier frequency domain by its power spectral density function $S_\varphi(f)$ (Walls and Allan, 1986; Jacques, 1978). The phase noise spectrum $S_\varphi(f)$ can analytically be expressed by a composite power law model:

$$S_\varphi(f) = h_{-2}f^{-4} + h_{-1}f^{-3} + h_0f^{-2} + h_1f^{-1} + h_2 \quad (1)$$

In Eq. 1, the coefficients h_{-2} to h_2 show contributions from: (1) random walk frequency noise, (2) frequency flicker noise, (3) white frequency noise, (4) flicker phase noise and (5) white phase noise, respectively (Walls and Allan, 1986; Jacques, 1978). In the time domain, phase noise is also conveniently characterized by Allan variance $\sigma_y^2(\tau_d)$ and $\sigma_y^2(\tau_d)$ can be expressed as:

$$\sigma_y^2(\tau_d) = \frac{4}{(\pi f_0\tau)^2}\int_0^\infty S_\varphi(f).\sin^4(\pi f\tau_d)df \quad (2)$$

Corresponding Author: Xie Xianming, College of Electronic Engineering, University of Electronic Science and Technology, Chengdu, China Fax: +86-28-83201545

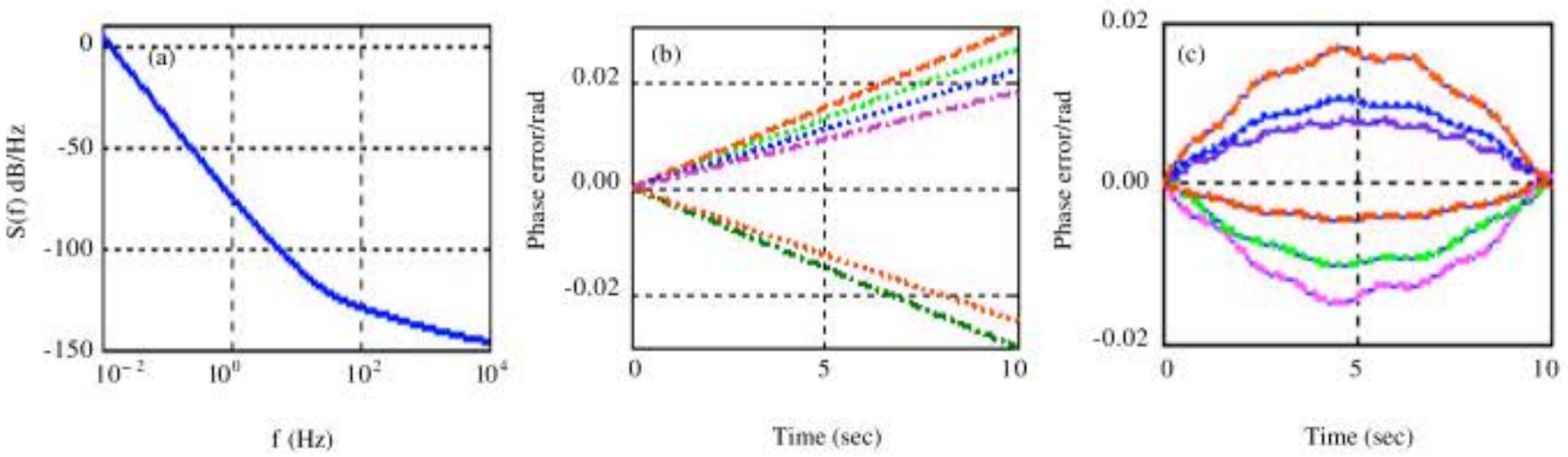

Fig. 1: Example of simulated oscillator phase errors (a) a phase noise spectrum $S_\varphi(f)$ of the typical oscillator (phase error spectrum), (b) linear errors (oscllator error) and (c) quadratic and high-frequency phase errors (oscillator phase error)

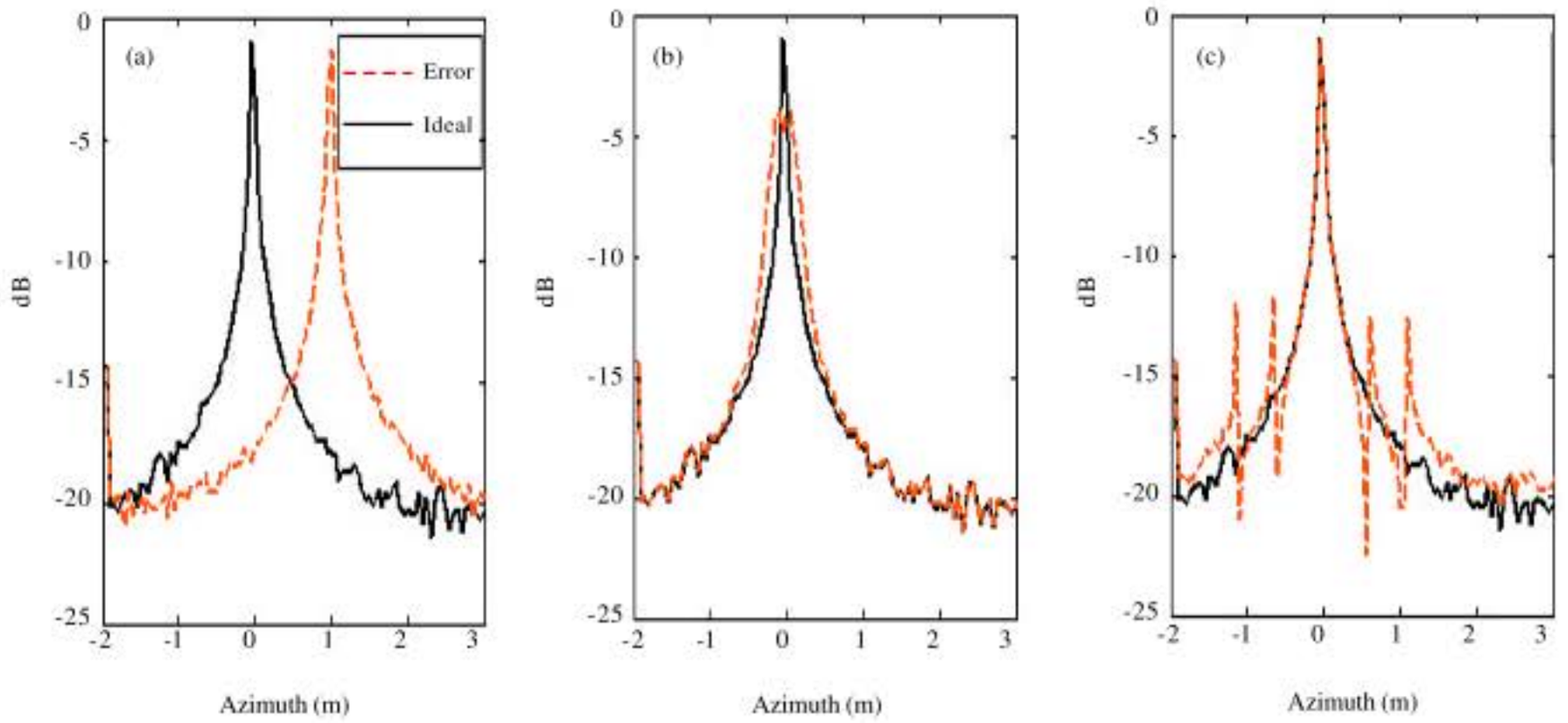

Fig. 2: Impact of the various phase noise in DBS imaging (a) azimuth shift, (b) broadening of impulse response and (c) spurious sidelobes

where, f_0 is the center frequency of the oscillator, τ_d is sample interval (Jiang and Lin, 2003).

Figure 1a-c show phase noise of the typical oscillator with the center frequency of f_{osc} ($h_{-2} = -75$ dB, $h_{-1} = -80$ dB, $h_0 = -125$ dB, $h_1 = 110$ dB, $h_2 = -150$ dB, $f_{osc} = 10^9$). Figure 1a shows a phase noise spectrum $S_\varphi(f)$ of the oscillator; Fig. 1b shows six 10s linear component of realization of the stochastic process shown in Fig. 1a and c show quadratic and high-frequency phase errors after subtraction of linear phase errors. In this study, frequency source phase noise parameter used in simulation is provided by Fig. 1a. Figure 2 shows that different phase noise will bring different effects on DBS images. Figure 2a shows azimuth shift caused by linear phase errors; Fig. 2b shows broadening of impulse response caused by quadratic phase errors; Fig. 2c shows spurious sidelobes caused by high-frequency phase errors.

RANGE WALKING CORRECTION AND AZIMUTH DECHIRPING

The resolution of the conventional DBS images is limited by range walking and azimuth chirping. Range walking correction technique and azimuth dechirping technique can increase the coherent accumulated time of DBS imaging system, which provides greater space for improving of the resolution of DBS images. Figure 3 shows geometry relation of radar and objection.

An equation of Doppler center f_{dc} estimation is provided in reference (Wang and Song, 2005).

$$f_{dc} = \frac{2v}{\lambda}\cos\alpha.\cos\beta \tag{3}$$

Where:

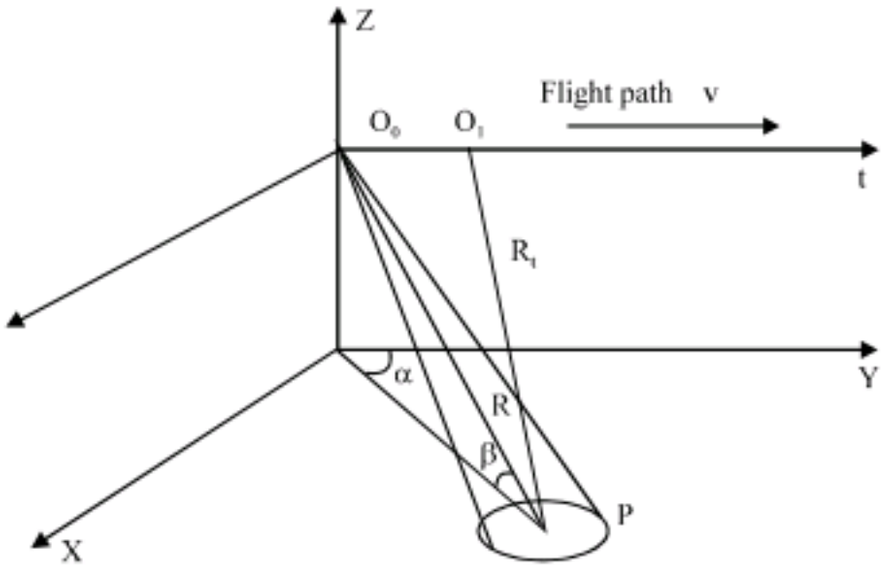

Fig. 3: Geometry relation of radar and objection

α = Azimuth angle
β = Elevation angle
ν = Velocity of the airplane
λ = Transmitted wavelength

The equation of frequency rate f_r is as follows:

$$f_r = \frac{2v}{\lambda R}(1-\cos^2\alpha\cos^2\beta) \quad (4)$$

Where:
R = Distance between radar and target scene

Range walking correction: Range walking correction function $RMC_{ref}(f, k)$ can be expressed as:

$$RMC_{ref}(f, k) = \exp(j2\pi f d_k) \quad (5)$$

Where:

$$d_k = \frac{\lambda f_{dc} k T_r}{c}$$

where, k is serial number of azimuth echo, T_r is pulse repetition cycle, c is light velocity. Let reference function of transmitted pulse is $R_{ref}(f)$. It is easy to correct the range walking by multiplying a correction coefficient $RMC_{ref}(f, k)$ by $R_{ref}(f)$ (Li *et al*., 2006), as shown in Fig. 4.

Azimuth dechirping: The aim of azimuth dechirping is canceling the quadratic phase so that the energy can centralize to one frequency point for one target. The way to perform azimuth dechirping is to multiply the signal by a reference signal (Li *et al*., 2006), as shown in Fig. 4.

Assume the raw signal after accumulating in the range direction is as follows:

$$S_a(R,k) = \exp(j2\pi f_{dc} t + j\pi f_r t_k^2) \quad (6)$$

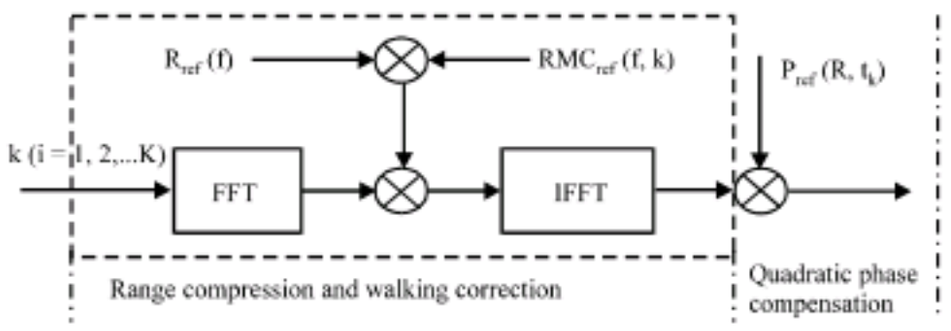

Fig. 4: Range compression walking correction and azimuth dechirping

Then, azimuth reference function can be expressed as:

$$P_{ref}(R,k) = \exp(-j\pi f_r t_k^2),\ t_k = kT_r \quad (7)$$

It can match the raw signal well enough to improve the resolution in the azimuth direction.

ANALYSIS OF PHASE ERROR IMPACT

Figure 5 is a DBS baseband signal model, where, f_{osc}, φ(t) is the nominal frequency and phase noise of the oscillator respectively; $m = f_0/f_{osc}$ is the frequency up-conversion factor and f_0 is the radar carrier frequency.

Phase errors $\varphi_B(t)$ in DBS baseband signal can be expressed as:

$$\varphi_B(t) = m[\varphi(t-\tau) - \varphi(t)] \quad (8)$$

where, τ is time delay.

Do autocorrelation of $\varphi_B(t)$ and can yield:

$$\begin{aligned} R_{\varphi_B}(t_1) &= E[\phi_B(t)\phi_B(t+t_1)] \\ &= E[m(\varphi(t-\tau)-\varphi(t))m(\varphi(t-\tau+t_1)-\varphi(t+t_1))] \\ &= m^2[2R_\phi(t_1) - R_\phi(t_1+\tau) - R_\phi(t_1-\tau)] \end{aligned} \quad (9)$$

where, the symbol E denotes mean operation

Taking the Fourier transform of $R_{\varphi_B}(t_1)$, the phase noise spectrum $S_{\varphi_B}(f)$ be expressed as:

$$S_{\varphi_B}(f) = 4m^2\sin^2(\pi f\tau)S_\varphi(f) \quad (10)$$

Analysis of linear phase error impact: Assume that Doppler frequency shift caused by linear phase error is κ, also further assume that azimuth angle shift is θ(κ). According to Eq. 3 and can yield:

$$\begin{aligned} f_{dc} + \kappa &= \frac{2v}{\lambda}\cos[\alpha+\theta(\kappa)]\cos\beta \\ &= \frac{2v}{\lambda}[\cos a\cos\theta(\kappa) - \sin a\sin\theta(\kappa)]\cos\beta \end{aligned} \quad (11)$$

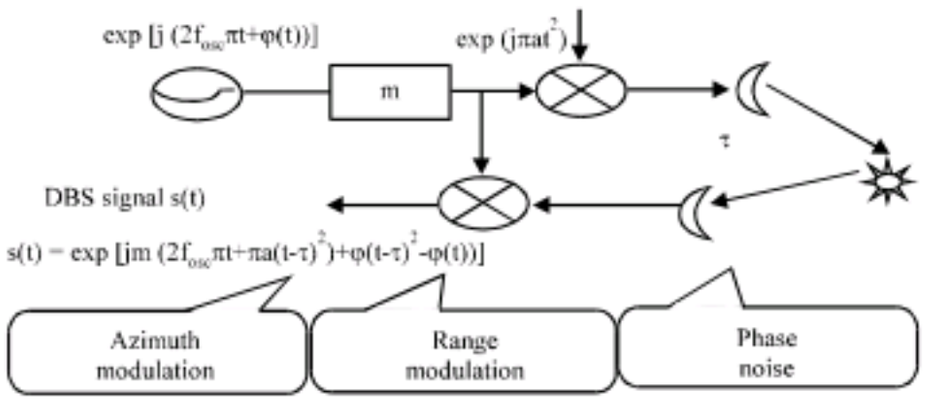

Fig. 5: DBS baseband signal model

Generally, $\theta(\kappa)<<1$ then, $\cos\theta(\kappa) \approx 1$ and $\sin\theta(\kappa) \approx \theta(\kappa)$ can yield:

$$f_{dc} + \kappa = \frac{2v}{\lambda}\cos a\cos\beta - \frac{2v}{\lambda}\theta(\kappa)\sin a\cos\beta \quad (12)$$

Substituting Eq. 3 into Eq. 12 yields:

$$\theta(\kappa) = \frac{\lambda}{2v\sin\alpha\cos\beta}\kappa \quad (13)$$

Then, azimuth shift distance can be expressed as:

$$d_a(\kappa) = \frac{\lambda R}{2v\sin\alpha\cos\beta}\kappa \quad (14)$$

where, κ is random variable, standard variance for $d_a(\kappa)$ can be expressed as:

$$\sigma_{d_a}^2 = \frac{(\lambda R)^2}{(2v\sin\alpha\cos\beta)^2}\sigma_\kappa^2 \quad (15)$$

In Eq. 15, σ_κ^2 is standard Variance for frequency shift κ.

According to study (Walls and Allan, 1986), has $\sigma_\kappa^2 = f_0^2\sigma_y^2(T_a)$.

Substituting Eq. 2 10 into Eq. 15 yields:

$$\begin{aligned}\sigma_{d_a}^2 &= \frac{(\lambda R)^2}{(2v\sin\alpha\cos\beta)^2} f_0^2 \frac{4}{(\pi f_0 T_a)^2}\int_0^\infty S_{\varphi_n}(f)\bullet\sin^4(\pi f T_a)df \\ &= \frac{4(\lambda R)^2 m^2}{(\pi v T_a \sin\alpha\cos\beta)^2}\int_0^\infty S_\varphi(f)\bullet\sin^6(\pi f T_a)df \\ &= \frac{4(cR)^2}{(\pi v T_a f_{osc}\sin\alpha\cos\beta)^2}\int_0^\infty S_\varphi(f)\bullet\sin^6(\pi f T_a)df\end{aligned} \quad (16)$$

where, the symbol • denotes multiplication operation, c is light velocity.

Resolution in azimuth direction:

$$\delta_a(R, T_a) = \frac{\lambda R}{2vT_a\sin\alpha\cos\beta} \quad (17)$$

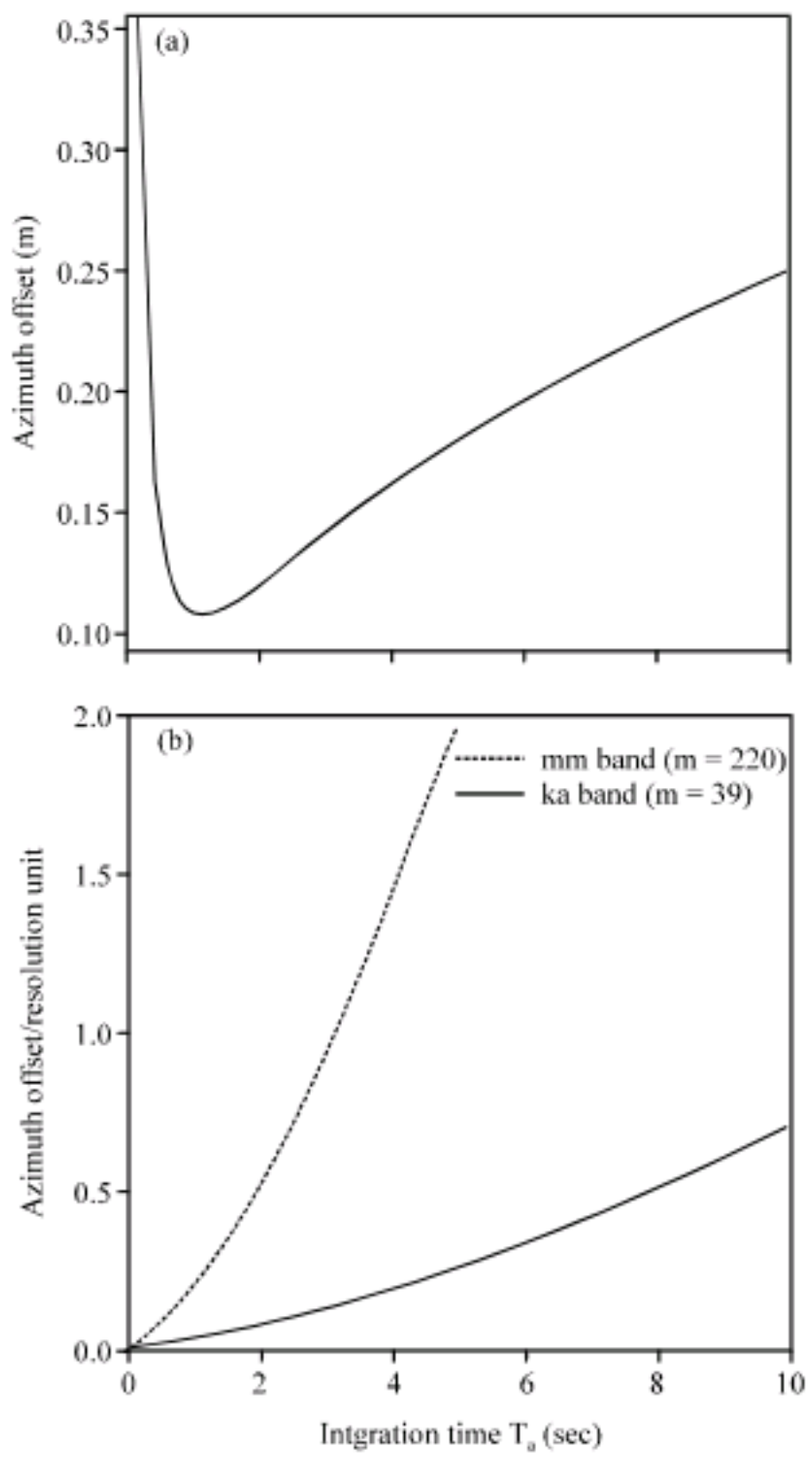

Fig. 6: Azimuth shift simulation (R = 50 km, $v = 10$ m sec^{-1}, $\alpha = 30°$, $\beta = 60°$) (a) shift in azimuth (unit/m) and (b) azimuth shift number of resolution unit

Then, shift number of resolution unit in azimuth direction:

$$D_a(\kappa) = \kappa T_a \quad (18)$$

Then, standard variance of shift number of resolution unit in azimuth direction:

$$\sigma_{D_a}^2 = T_a^2\sigma_\kappa^2 = T_a^2 f_0^2\sigma_y^2(T_a) = \frac{16m^2}{\pi^2}\int_0^\infty S_\varphi(f)\bullet\sin^6(\pi f T_a)df \quad (19)$$

Figure 6a models the shift in azimuth direction. It is shown from Fig. 6 that the azimuth shift firstly decreases with the coherent accumulated time increasing and about 1 sec with the smallest shift. However, the azimuth shift increases with the coherent accumulated time increasing when the coherent accumulated time more than 1 sec. Figure 6b estimates azimuth shift number of resolution

unit. It is shown from Fig. 6b that the shift number increases with the coherent accumulated time increasing and the shift in mm band is larger than in Ka band. It can be concluded from Fig. 6 that increasing coherent accumulated time may result in larger azimuth shift.

Analysis of quadratic phase error impact: Quadratic phase errors of oscillator basically meet the form of a quadratic function of time in a coherent accumulated time. Quadratic phase errors result in broadening of spectrum function and decline of main lobe, as well as enhancing of sidelobes.

Assume frequency rate caused by quadratic phase error is u. In a coherent accumulated time, the largest quadratic phase error:

$$\Omega = \pi u(\frac{T_a}{2})^2$$

According to the study (Jacques, 1978), frequency rate u can be expressed as:

$$u = \frac{d(d\varphi_B(t))}{2\pi dt^2}$$

then, has

$$\sigma_u^2 = (2\pi)^2 f^4 S_{\varphi_B}(f) \quad (20)$$

Standard variance of biggest quadratic phase error can be expressed as:

$$\sigma_{\varphi_q}^2 = \pi^2(\frac{T_a}{2})^4\sigma_u^2 = \pi^4 T_a^4 \int_0^{1/T_a} f^4 m^2 S_\varphi(f)\sin^4(\pi T_a f)df \quad (21)$$

Figure 7 estimates quadratic phase errors σ_{φ_q} (unit, π) in mm band and in Ka band. A typical requirement for quadratic phase errors is $\sigma_{\varphi_q} \le 0.5\pi$, which would enable a maximum coherent accumulated time T_a of approximately 2.5 sec in mm band and 8 sec in Ka band.

Analysis of high-frequency phase error impact: Usually, high-frequency phase error circle is less than a coherent accumulated time. High-frequency phase errors result in spurious sidelobes, which may seriously impact the quality of DBS images (Pi and Yang, 2007). This deterioration can be characterized by an increase of the integrated sidelobe ratio (ISLR), which measures the energy in the sidelobes relative to the energy in the main lobe. The deterioration of the ISLR may be approximated as:

$$ISLR_h = 4m^2 \int_{1/T_a}^{\infty} S_\varphi(f)\sin^4(\pi f T_a)df \quad (22)$$

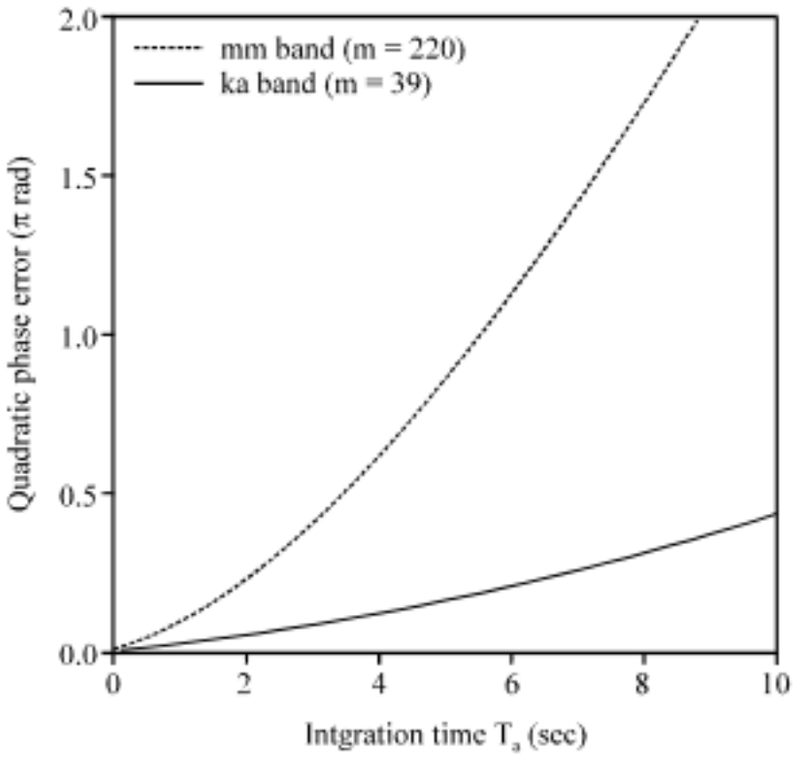

Fig. 7: Estimates of quadratic phase error

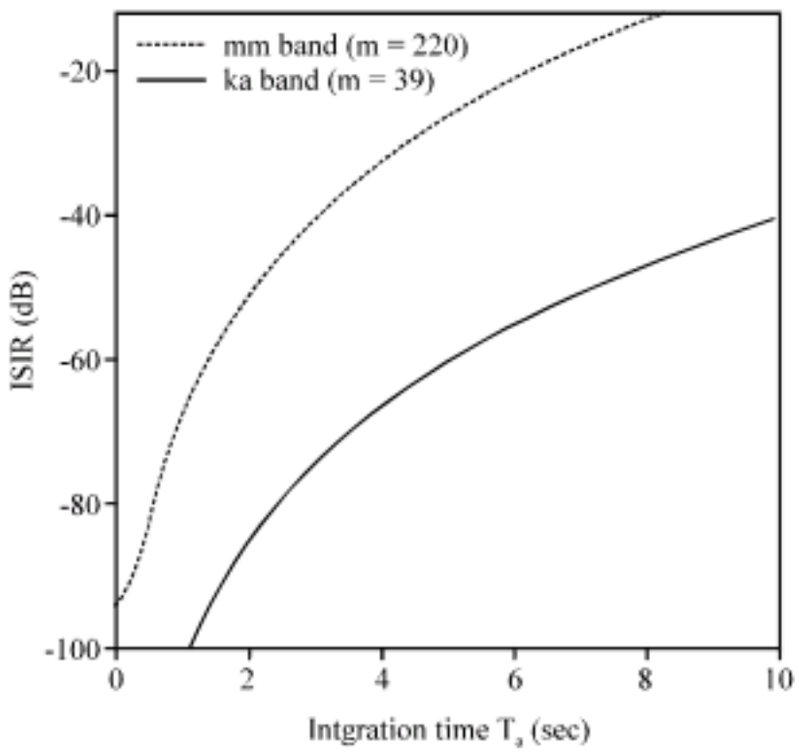

Fig. 8: Estimates of ISLR

Figure 8 estimates the ISLR for high-frequency phase errors. It can be conclude from Fig. 8 that the ISLR increases with the coherent accumulated time increasing. A typical requirement for high-frequency phase errors is ISLR <-35 dB, which would enable a maximum coherent accumulated time T_a of approximately 2.5 sec in mm band and 8 sec in Ka band.

DISCUSSION

In ideal case, according to Eq. 16, the azimuth resolution of DBS images is expressed as:

$$\delta_a(R,T_a) = \frac{\lambda R}{2vT_a \sin\alpha\cos\beta}$$

Obviously, it is mainly determined by several parameters including transmitted wavelength λ, azimuth

angle α, elevation angle β, velocity of the airplane v, coherent accumulated time T_a.When λ, α, β and R, as well as v keep constant, $\delta_a(R, T_a)$ is mainly determined by coherent accumulated time T_a and decreases with coherent accumulated time increasing, which shows that the azimuth resolution can be improved with coherent accumulated time increasing.

However, it is shown from Fig. 6 that the azimuth shift caused by phase noise increases with coherent accumulated time increasing. For a single target, the shift has no impact on the quality of DBS images. In actual imaging, the shift of all targets in all direction is random, which results in distortion of the images.

It is also shown from Fig. 7 and 8 that quadratic phase errors (σ_{φ_i}) and integrated sidelobe ratio (ISLR) also increase with the coherent accumulated time increasing, which shows a long coherent accumulated time may degrade the resolution of DBS images.

In earlier studies, such as study (Tobin, 1996; Qi and Zhuizhen, 2004), the coherent accumulated time is mainly limited by several factors including range walking and azimuth chirping. So, in the conventional DBS imaging, the coherent accumulated time is very short. For a short coherent accumulated time, impact of frequency source phase noise is very small and it can be ignored.

In high-resolution DBS imaging, range walking and azimuth chirping is compensated, which may acquire a long coherent accumulated time. From the above analysis, we know that impact of frequency source phase noise may be very serious in higher-resolution DBS imaging with a long coherent accumulated time.

Therefore, the selection of coherent accumulated time should be paid more attention in high-resolution DBS imaging. A long coherent accumulated time is necessary for high-resolution DBS imaging, but also the impact of phase noise also should be considered.

CONCLUSION

The effects of frequency source noise on the resolution Of DBS imaging system is obvious. The azimuth shift and the broadening of spectrum function caused by frequency source phase noise, as well as the deterioration of integrated sidelobe ratio (ISLR) increase with the coherent accumulated time increasing. Therefore, the length of coherent accumulated time will be influenced by frequency source phase noise. A short coherent accumulated time will inevitably degrade the resolution of system. However, for a long coherent accumulated time, frequency source phase noise will bring serious impact on the quality of DBS images. One way to solve this problem is improving stability of frequency source.

It is also concluded from Fig. 7 and 8 that the impact of frequency source phase noise in different frequency band is not the same. DBS imaging systems operating in higher frequency band will suffer more impact and should be paid more attention.

ACKNOWLEDGMENT

This research was supported by the National Natural Science Foundation of China under Grants No. 60772143.

REFERENCES

Cheng, Y. and S. Changyin, 2000. Applications of superresolution signal estimators to doppler beam sharpened imaging. Dianzi Kexue, 22: 392-397.

Gerhard, K. and M. Younis, 2006. Impact of oscillator noise in bistatic and multistatic SAR. IEEE Geosci. Remote Sens., 3: 424-427.

Jacques, R., 1978. Characterization of phase and frequency instabilities in precision frequency sources. Proc. IEEE, 66: 1048-1075.

Jiang, P. and Z. Lin, 2003. Relation between radar improved factor with phase noise and allan variance. J. Astronautic Metrol. Measurment, 23: 52-56.

Li, Y., X.M. Dao and B. Zheng, 2006. DBS imaging and GMTI in a wideband airborne mechanic scanning radar. Xi'an Dianzi Keji Daxue Xuebao, 33: 116-120.

Mao, S. and L. Shaohong, 2000. Study of real-time image by DBS on airborne PD radar. Acta Electronica Sinica, 28: 32-34.

Pi, Y. and Y. Jianyu, 2007. Synthetic Aperture Radar Imaging Theory. House of University of Electronic Science and Technology of China, Chengdu, ISBN: 978-7-81114-412-3.

Qi, J. and W. Zhuizhen, 2004. Optical and radar remote sensing cooperation and applications in agriculture. Dianbo Kexue Xuebao, 19: 399-404.

Tobin, M., 1996. Real time simultaneous SAR/GMTI in a tactical airborne environment. Proceedings of the European Conference on Synthetic Aperture Radar, 1996, Germany, pp: 63-66.

Walls, F. and D. Allan, 1986. Measurements of frequency stability. Proc. IEEE, 74: 162-168.

Wang, H. and W. Song, 2005. High resolution DBS imaging and moving target trajectory processing. Dianbo Kexue Xuebao, 20: 637-641.

Wei, S. and S. Wen, 2005. High resolution image by DBS with SAR/GMTI. Infrared Laser Eng., 34: 337-340.

Younis, M., R. Metzig and G. Krieger, 2006. Performance prediction of a phase synchronisation link for bistatic SAR. IEEE Geosci. Remote Sens., 3: 466-469.

Zhang, Z., 1991. Discussion of Doppler Beam Sharpening (DBS) theoretical and practical problems. Modern Radar, 13: 1-12.

Zhou, Y., 1988. Airborne pulse doppler radar DBS technology. Aviat. J., 9: 574-581.